Available online at www.sciencedirect.com
ScienceDirect
Ceramics International 36 (2010) 443–450
CERAMICS INTERNATIONAL
www.elsevier.com/locate/ceramint

Preparation of oriented SiO_3^{2-} doped TiO_2 film and degradation of methylene blue under visible light irradiation

Xiangying Xu, Dehong Yin *, Shufeng Wu, Jinqu Wang, Jinming Lu

State Key Laboratory of Fine Chemicals, Institute of Adsorption and Inorganic Membrane, Department of Chemical Technology, Dalian University of Technology, Dalian 116012, China

Received 7 May 2009; received in revised form 12 June 2009; accepted 16 August 2009
Available online 23 September 2009

Abstract

SiO_3^{2-} doped TiO_2 films with oriented nanoneedle and nanorectangle block structure has been firstly synthesized by hydrothermal synthesis method. The prepared samples are characterized, X-ray diffraction (XRD) results demonstrate that the SiO_3^{2-} doped TiO_2 films are rutile and brookite phases. The scanning electron microscope (SEM) analysis reveals that the quantity of O_2 affects the morphology of the SiO_3^{2-} doped TiO_2 films (SiTiA films prepared with unmodified substrate). The SiO_3^{2-} doped TiO_2 films (SiTiB films prepared with modified substrate) display two layers, one is porous structure, the other is nanoneedle structure. UV–vis, IR, transmission electron microscopy (TEM) and energy-dispersive X-ray (EDX) microscopy all prove that SiO_3^{2-} have been doped in the TiO_2 crystal structure. They have remarkable red shift and higher photocatalytic activity of degradation of methylene blue than P-25 under visible light ($\lambda > 420$ nm) irradiation. Besides, photocatalytic activity of the film is stable during 4 times recycling.

Keywords: SiO_3^{2-} doped TiO_2 films; Hydro-thermal synthesis methord; Photocatalytic activity; Red shift

1. Introduction

Titanium dioxide (TiO_2) has been extensively used as the photocatalytic material due to its self-cleaning [1–4], purifying [5–7] and antibacterial [8,9] properties. Photocatalytic degradation of remanent chemical contaminants in waste water and atmosphere on TiO_2 surface under UV irradiation offers an effective approach to settle various environmental problems [10,11]. However, the reactivity of TiO_2 mostly relies on UV light while there is only 5% UV light in the solar spectrum, which enormously limits the using efficiency of sunlight [12,13]. Harvesting more sunlight for photocatalytic or photoelectrochemical purposes will be enormously enhanced by extending the photoresponse of TiO_2 into the visible spectral range.

Recent theoretical and experimental studies have shown that the desired band gap narrowing of TiO_2 can be achieved using nonmetal atoms dopants to enhance the photoactivity of TiO_2 in the visible spectral range, such as N [14,15], I [16,17], and S [18]. Gole [15] prepared catalytically active $TiO_{2-x}N_x$ structured particles whose absorption onset extended well into the visible region at 550 nm. Sandro et al. [16] prepared $(I_2)_n$ encapsulation inside TiO_2 that a broad absorption band appeared in the interval between 400 nm and 667 nm. However, there has been few reports on the modification of TiO_2 with acid radical, such as SiO_3^{2-}, to achieve red shift.

Furthermore, the application of powdered TiO_2 as a photocatalyst in wastewater treatment had the drawback of post-separation in a slurry system after photoreaction. Therefore, attempts have been made to immobilize the TiO_2 in the form of thin films on different rigid substrates, such as glass [19,20] which is available and possesses good light-admitting quality substrate and quartz [21]. Bolunt et al. [19] prepared transparent thin-film TiO_2 layer by sol–gel deposition method on Pyrex reactor which was showed to be more active for photocatalytic oxidation of acetaldehyde, acetic acid and toluene than Degussa P-25 thin films under UV light. Mi et al. [21] prepared N-doped TiO_2 films on quartz by calcining the TiO_2 films in ammonia atmosphere. Eiji et al. [22] firstly reported an evolution of a new morphology of film consisting of

* Corresponding author. Tel.: +86 411 8292 0545; fax: +86 411 8363 3680.
E-mail address: yindehong2010@163.com (D. Yin).

0272-8842/$36.00
doi:10.1016/j.ceramint.2009.09.011

highly crystalline (nearly single-crystalline) rectangular parallelepiped rutile TiO_2 in a submicrometer scale. It is regretful that there was no application for the films.

In this paper, SiO_3^{2-} doped TiO_2 films were firstly fabricated by one simple step without using any templates or additives which was easy to be applied in practice. The films are beautiful with oriented nanorectangle block and nanoneedle structure. UV–vis, IR, TEM and EDX all prove that SiO_3^{2-} have been doped in the TiO_2 crystal structure.

2. Experimental

2.1. Treatment of subtrates

The glass slides were treated as substrates with two different ways. One way, the glass slides were cleaned with deionized water and unmodified. The SiO_3^{2-} doped TiO_2 films which were prepared with this kind of substrates denoted as SiTiA films. Another way, the glass slides were cleaned with 1.0 M HCl and ethanol solution in an ultrasonic bath. After dried at 373 K, the glass slides were placed in Teflon-lined autoclaves which were filled with deionized water. Then the autoclaves were heated at 448 K for 8 h. After hydrothermal treatment, the glass slides were washed with deionized water several times and dried at 308 K [23]. The SiO_3^{2-} doped TiO_2 films which were prepared with this modified substrates denoted as SiTiB films.

2.2. Preparation of SiO_3^{2-} doped TiO_2 films

The SiO_3^{2-} doped TiO_2 films were synthesized via hydrothermal treatments of aqueous titanium trichloride ($TiCl_3$; 6 mL) solution and sodium silicate ($NaSiO_3$; 0.060 M) solution. The solutions and previous treated substrates were placed in Teflon-lined autoclaves which were filled with a certain amount of O_2. Then Teflon-lined autoclaves were heated at 473 K for typically 4 h. The resultant films were rinsed with deionized water and dried at 308 K (the film noted as SiTi film).

2.3. Characterization

The structure and phase identification were characterized by X-ray diffraction (XRD) patterns which were recorded on D/Max Rigaku diffractometer using Cu Kα radiation ($\lambda = 0.1542$). The surface morphologies were examined by scanning electron microscope (SEM, KYKY-2800B). The samples were coated with gold to make conducting before put into the SEM chamber. The film segments scraped from the glass slides were characterized by transmission electron microscopy (TEM) with an energy-dispersive X-ray spectrometer (a Tecnai G^2 F30 S-Twin transmission electron microscopy). FTIR spectras of SiO_3^{2-} doped TiO_2 were measured to investigate structural information and specific molecule-groups information (a Bruker EQUINOX55 spectrometer). UV–vis diffuse spectra were obtained on a JASCO V-55O spectrometer with $BaSO_4$ for reference.

2.4. Measurement of photocatalytic activity

The photocatalytic activity of the samples was evaluated by photodegrading methylene blue, because methylene blue was one of the most typical persistent organic pollutants. Photocatalytic experiments were carried out in a homemade reactor which was surrounded by a cooling system to keep room temperature of the reaction system. A 300-W iodine tungsten lamp was used as the light source and photocatalytic activity of SiO_3^{2-} doped TiO_2 films were tested by visible light that any irradiation below 420 nm was removed by a cutoff filter. Photodegradation of methylene blue (20 mg/L) was carried out in a jacketed cylinder which was stirred by a magnetic stirrer in the below and illuminated in the right. The distance between light source and the surface of the solution was 16 cm. The solution was kept in the dark for 0.5 h to establish an adsorption–desorption equilibrium before the visible light radiation. The concentration of the methylene blue solution was determined on the basis of its characteristic optical absorption at 665 nm on a 721 spectrophotometer.

3. Results and discussion

3.1. XRD analysis

Fig. 1 shows the X-ray diffraction (XRD) pattern of the SiTiA film. The crystalline phases are confirmed rutile and brookite [22]. All the diffraction peaks agree with those of TiO_2 in the rutile and brookite forms, meanwhile the [1 1 0] and [1 0 1] axises of SiTiB film are enhanced. The difference in the peak intensity ratio is caused by orientation.

3.2. SEM analysis

Fig. 2 shows scanning electron microscope (SEM) images of SiTi films. The morphology of the SiTiA film (Fig. 2b) appears to be nanorectangle block which was prepared with a little of O_2. Surprisingly the morphology is changed to be nanoneedle (Fig. 2a) when it was prepared with a lot of O_2. So these results

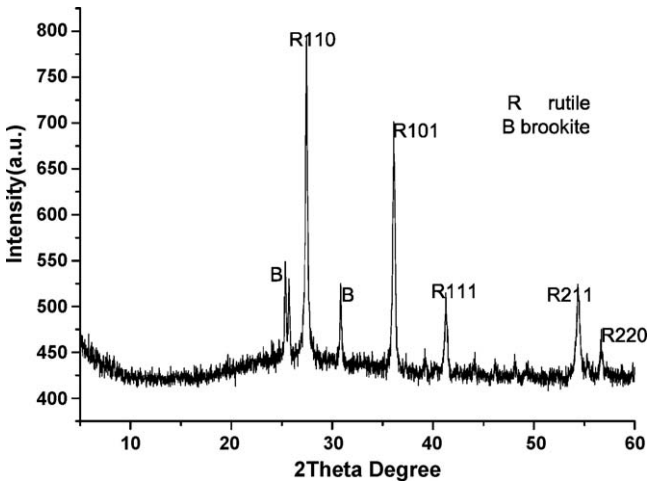

Fig. 1. XRD pattern of the sample SiTiA film.

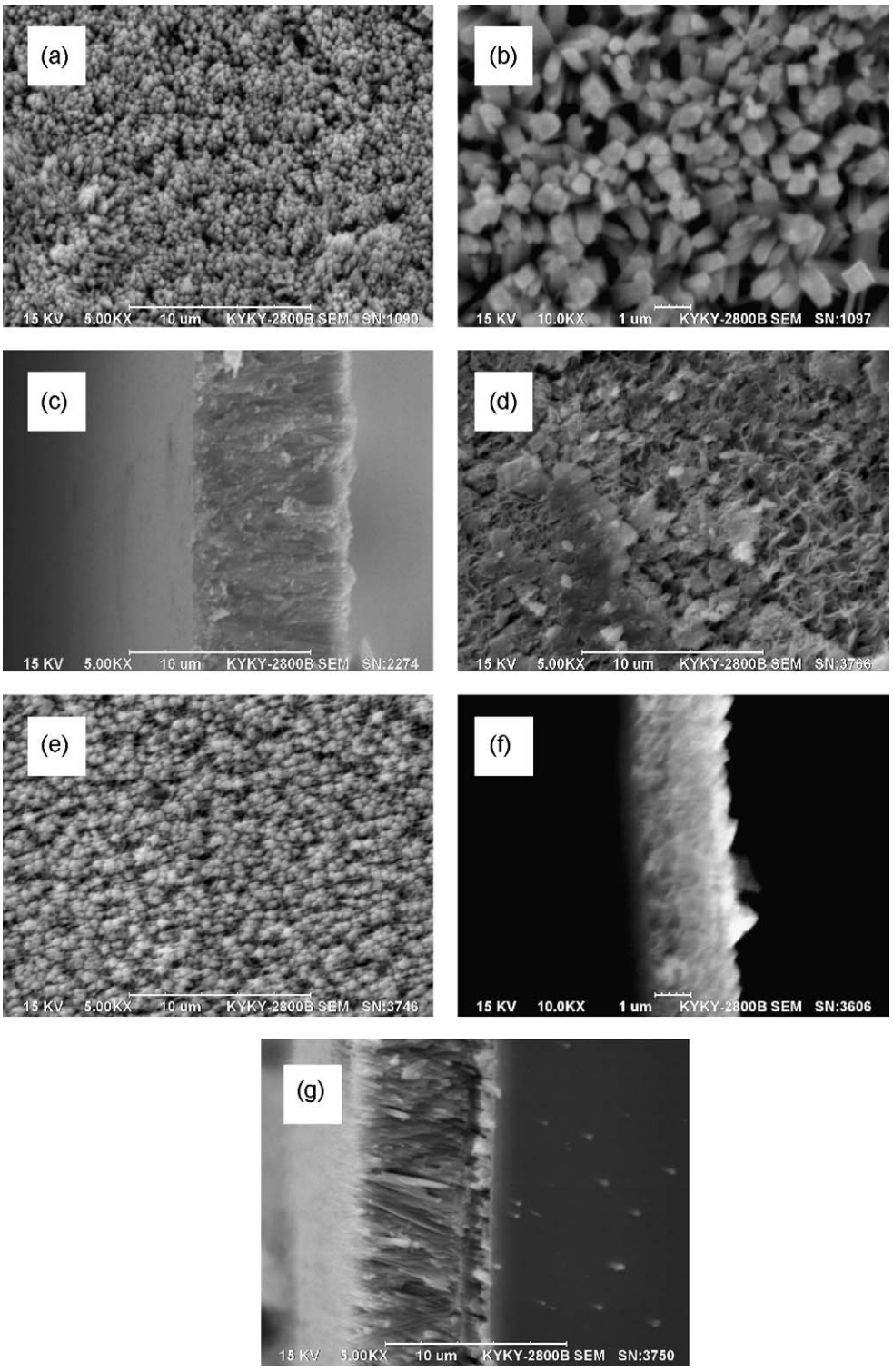

Fig. 2. SEM images of the SiO_3^{2-} dopedTiO_2 film. (a and c) SiTiA film prepared with a lot of O_2. (b) SiTiA film prepared with a little of O_2. (d and f) The film formed by treating glass with hydrothermal synthesis. (e and g) SiTiB film prepared with a lot of O_2.

show that the quantity of O_2 affects the morphology of the SiTiA films. And with O_2 increasing, the nucleations become more on some spots of the substrate surface, resulting to grow nanoneedle which takes up less area. Besides, as shown in Fig. 2c, the SiO_3^{2-} doped TiO_2 film tightly grows perpendicularly on the glass substrate and the thickness is approximately 8 μm, which is enough thick to acquire visible light and induce photoproduction electron and photoproduction hole. The cross-section of the film appears to be oriented and vicelike which is still tight on the substrate after 4 times recycling. The probable reason is that SiO_3^{2-} in TiO_2 film has successfully formed Si–O–Si bonds with Si in the glass. At the same time, as shown in

Fig. 2d and f, the film fabricated by modified glass substrate with hydrothermal synthesis displays porous structure and the thickness of the film is about 2 μm. According to Ho et al. [23], the chemical composition analysis using energy-dispersive X-ray (EDX) spectroscopy illustrates that the film mainly contain Si, O, Ca, Al and Mg, without Na which was instead in the process of hydrothermal synthesis. The SiTiB film (Fig. 2e) which was prepared with a lot of O_2 also appears to be nanoneedle structure and the thickness of film is about 8 μm (Fig. 2g). The thickness of SiO_3^{2-} doped TiO_2 film is approximately 6 μm and the interface of two layers is evident.

The SEM analysis reveals that the quantity of O_2 affects the morphology of the SiTiA films and the TiO_2 nanocrystals have preferred orientation with most of their tips roughly pointing upward. Moreover, significantly enhanced peaks of both (1 1 0) and (1 0 1) reflections further confirm that a preferred [0 0 1]-oriented SiO_3^{2-} doped TiO_2 film is perpendicular to the substrate. The SiTiB films with modified substrate display two layers, one is porous structure, the other is nanoneedle structure.

3.3. FTIR analysis

The Fourier transform infrared absorption (FTIR) spectra of SiTiA film and P-25 (Degussa) are shown in Fig. 3. It is reported that the high-frequency part of the spectra is dominated by the OH stretching vibration (3100–3500 cm^{-1}) and bending vibration (1640 cm^{-1}) of water. The peaks at about 2920 cm^{-1}, 600–700 cm^{-1}, 1110 cm^{-1} correspond to Ti, Ti–O and unsymmetry stretching vibration of Si–O–Si, respectively. Two absorption bands near 1036 cm^{-1} and 930–970 cm^{-1} can be ascribed to the stretching vibration of SiO_3^{2-} and Ti–O–Si respectively [24–26]. The above results illustrate that SiO_3^{2-} phase doped in TiO_2 matrix and form partially Ti–O–Si group in the matrix of TiO_2.

3.4. UV–vis diffuse spectra analysis

Fig. 4 illustrates the UV–vis diffuse reflection spectra of sample SiTiA film, P-25 (Degussa) and glass (substrate). The

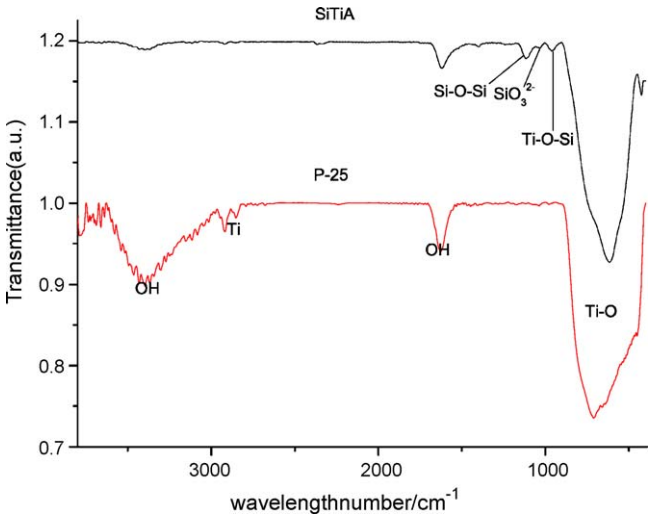

Fig. 3. FTIR spectra of sample SiTiA film and P-25 (Degussa).

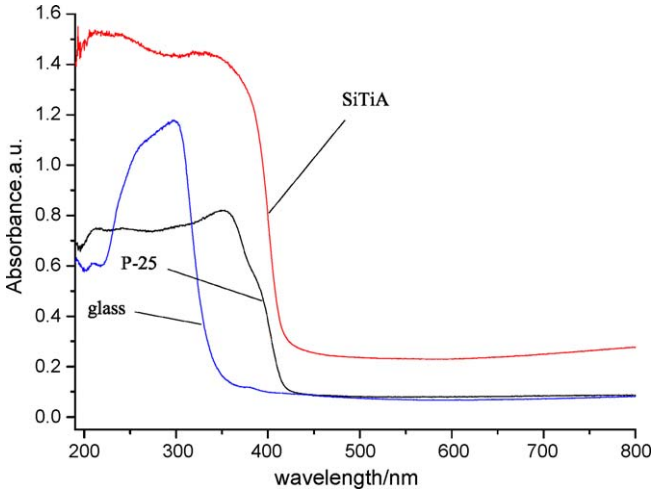

Fig. 4. UV–vis diffuse spectra of SiTiA film, P-25 and glass.

synthesized sample SiTiA films demonstrate more drastic and stronger photoabsorption in the visible light range from 400 to 550 nm than P-25. SiO_3^{2-} doped TiO_2 film can shift the absorption edge of TiO_2 to the visible light range and narrow

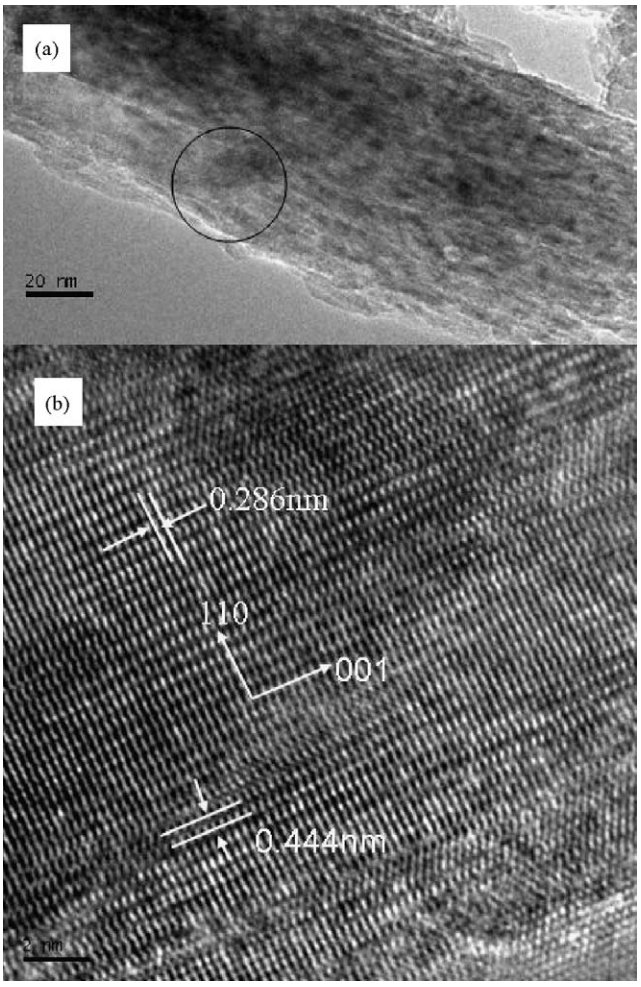

Fig. 5. TEM images (a) a low magnification image of SiTiA film prepared with a lot of O_2 and (b) a high-resolution transmission electron microscope (HR-TEM) image of SiTiA film.

the band gap. Zhang et al. [27] reported the small blue shift of 20% silica/TiO_2 composite membrane. That mainly ascribed to the formation of small TiO_2 particles by embedding of amorphous silica into the TiO_2 matrix. Zhang et al. [26] also reported the SiO_2-doped TiO_2 appeared to be obvious blue shift in the absorbing band edge. Here, from the UV–vis diffuse spectra, it has remarkable red shift so further confirms SiO_3^{2-} doped in TiO_2 crystal structure and excludes mechanical mixture of TiO_2 with SiO_2. The absorption intensity of SiTiA film was obviously higher than that of P-25, which would be beneficial for photocatalytic degradation of organic pollutants under visible light irradiation [27].

3.5. TEM analysis

Fig. 5 shows transmission electron image of SiTiA films. A low magnification of SiTiA film prepared with a lot of O_2 is showed in Fig. 5a corresponding to it is high-resolution transmission electron (Fig. 5b). The distances between the adjacent lattice fringes can be assigned to the interplane distance of rutile TiO_2 (0 0 1) and (1 1 0), which are $d_{0\,0\,1} = 0.286$ nm and $d_{1\,1\,0} = 0.444$ nm. The latter Lattice distance is bigger than pure TiO_2 $d_{1\,1\,0} = 0.325$ nm. It is ascribed to SiO_3^{2-} doped in TiO_2 crystal structure. The [1 1 0] axis was perpendicular to the wall. The crystals therefore grew along the [0 0 1] axis, which was perpendicular to the [1 1 0] axis. These findings explain the above-mentioned orientation of the film according to XRD and SEM results. SiO_3^{2-} doped TiO_2 film appears to be nanoneedle in Fig. 6a. EDX (energy dispersive X ray fluorescence) image of SiTiA film (Fig. 6c which is corresponding to the area in Fig. 6a) reveals that there is only Si element in TiO_2 crystal structure and free from Na or Cl element which further proves that SiO_3^{2-} have been doped in the TiO_2 crystal structure. Copper ions come from the copper web. Fig. 6d and e are EDX energy maps of Ti element and Si element respectively corresponding to Fig. 6b. The distribution of Si element is similar to the distribution of Ti element. Si element is essentially dispersed in TiO_2, not get together.

3.6. Mechanism

The probable chemical reaction mechanism is as follow: $TiCl_3$ quickly hydrolyzes into $TiOH^{2+}$ when it mixed with H_2O (1) [22]. Then adding $NaSiO_3$, $TiOH^{2+}$ reacts with it and forms $Ti^{2+}OSiOONa$ (2). Since $TiOH^{2+}$ space resistance is very small, it has chance for SiO_3^{2-} to form Si-O-Ti bond. Although Ti (III) is slowly oxided to Ti (IV) by O_2 at 473 K, Ti–O–Si bond is still stable, meanwhile combing with glass substrate, ultimately forming SiO_3^{2-} doped TiO_2 film on the substrate (3) [28]. Without $NaSiO_3$, the tightly and orientedly TiO_2 film is difficult to form and easy to be polished off. When $NaSiO_3$ is replaced by $NaS_2O_3{\cdot}5H_2O$, KNO_3 or $NaIO_3$, the TiO_2 film is also difficult to form. The above results illustrate that $NaSiO_3$ is the appropriate choice in fabricating the film. These SiO_3^{2-} ions likely serve as the nucleation sites for the rutile crystals. Based on the titanyl silicate structure, the silicate tetrahedra prefers binding to the vertexes of the Ti–O octahedral [28]. The latter group of negative ions is easy to acquire electron, $TiCl_3$ mixed with them, Ti (III) is quickly changed to Ti (IV). Moreover, the film could not be fabricated when using aqueous $TiCl_4$ solution under the same experimental conditions. When using Ti (IV) instead of Ti (III) as the Ti source, it quickly hydrolyzes into $Ti(OH)_4$ when mixed with H_2O (4). And $Ti(OH)_4$ space resistance is very great. Even though reacting with $NaSiO_3$, it is not stable and easily removes H_2O molecule and forms TiO_2 crystal when it is heated (5). Another important point, gradual growth is necessary for the formation of crystal system. The rate of reaction of Ti (IV) in forming TiO_2 is too fast to permit to control thermodynamic equilibrium to be attained [29].

So the film could not be fabricated when using aqueous $TiCl_4$ solution under the same experimental conditions. The film deposition is found to be promoted in the oxygen-saturated solution, while the nitrogen saturated solution can not lead to the formation of the rutile film [22]. The process of Ti (III) being slowly oxided into Ti (IV) by O_2 well controls supersaturation. So that SiO_3^{2-} doped TiO_2 films is successfully fabricated. In a word, Ti (III), stable acid radical and O_2 are the crucial elements in fabricating the film.

$$Ti^{3+} + H_2O = TiOH^{2+} + H^+ \quad (1)$$

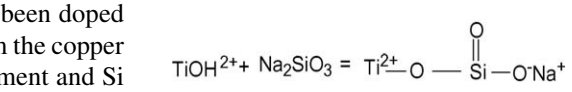

(2)

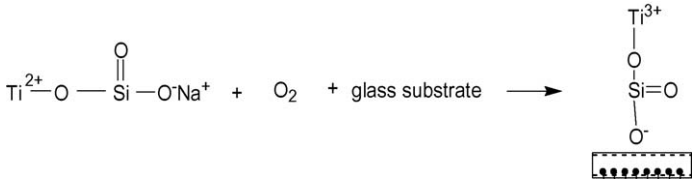

(3)

$$Ti^{4+} + 4H_2O = Ti(OH)_4 + 4H^+ \quad (4)$$

$$Ti(OH)_4 = TiO_2 + 2H_2O \quad (5)$$

3.7. Photocatalytic properties of SiTi films

In this report, the photocatalytic properties of SiTiA film and SiTiB film were examined. Fig. 7 shows the area of film on the substrate. When the substrate was placed in the Teflon-lined autoclave, only the area of 4.5 cm × 2.5 cm was immerged in the reactive solution. When it was took out form the Teflon-lined autoclave after 473 K for 4 h, the area of 3.3 cm × 2.5 cm

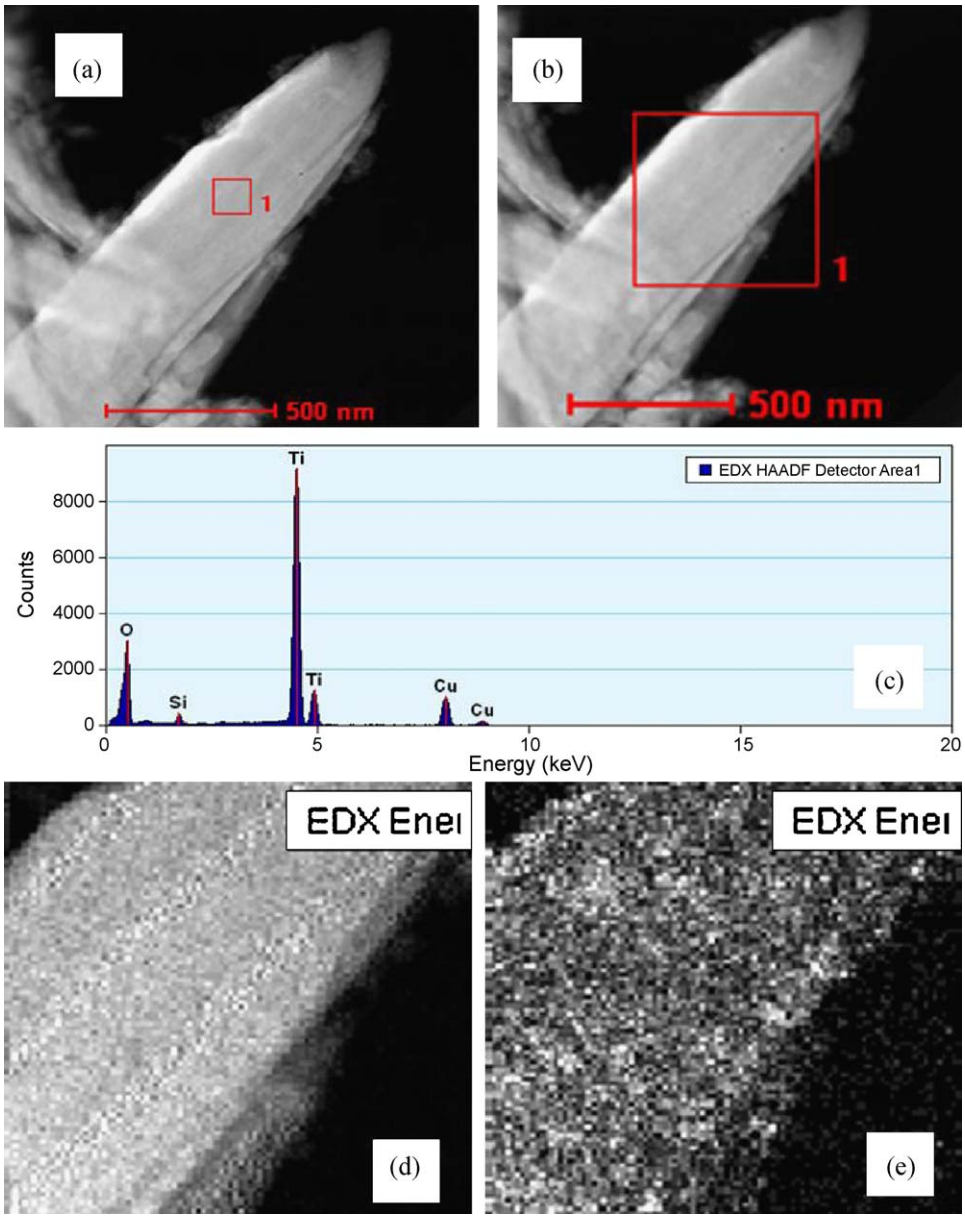

Fig. 6. STEM and energy-dispersed X-ray (EDX) spectroscopy images of SiTiA film. (a) STEM image of SiTiA film, (b) STEM image of SiTiA film, (c) EDX image of SiTiA film corresponding to (a), (d) EDX energy map of Ti corresponding to (b), (e) EDX energy map of Si corresponding to (b).

grew film. The bottom substrate was difficult to form film, because the bottom O_2 was deficient moreover there was much precipitation covered the substrate. As a result, the effective photocatalytic area of film was approximately 3.0 cm × 2.5 cm (Fig. 7).

To compare the photocatalytic activity of commercial TiO_2 (P-25), SiTiA film and SiTiB film, photodegradation of methylene blue as a test reaction was performed according to procedure reported in the literature [30]. 0.06 g P-25 photocatalyst was suspended in 60 mL metheylene blue solution (20 mg/L) under stirring magnetically, while SiTi film with the area of 3.0 cm × 2.5 cm immersed in 60 mL metheylene blue solution (20 mg/L) under stirring magnetically. Under visible light ($\lambda > 420$ nm), samples of SiTiA (Fig. 8b) and SiTiB (Fig. 8c) shows much better photocatalytic activity than P-25 (Fig. 8d). The difference in photocatalytic activity between P-25 and SiTi films can be ascribed to greatly high absorbance in the visible light range (between 420 and 550 nm) of the latter, although there is wide gap of surface area between them ($51\ m^2\ g^{-1} \times 0.06\ g = 3.06\ m^2$ for P-25 which can full contacted with methylene blue in powder vas $0.03\ m \times 0.025\ m = 0.00075\ m^2$ which is the area of substrate covered with SiTi film for the latter). The superiority of SiTi film is ascribed to greatly high absorbance in the visible light range (between 420 and 550 nm) which plays a crucial role in the experiments. The photocatalytic activity of SiTiA film (Fig. 8b) and SiTiB film (Fig. 8c) is same. A porous structure actually enlarge surface area of substrate. Due to the morphology of SiO_3^{2-} doped TiO_2 film is nanoneedle, the surface area of film has not been greatly enlarged. Besides the thickness of the

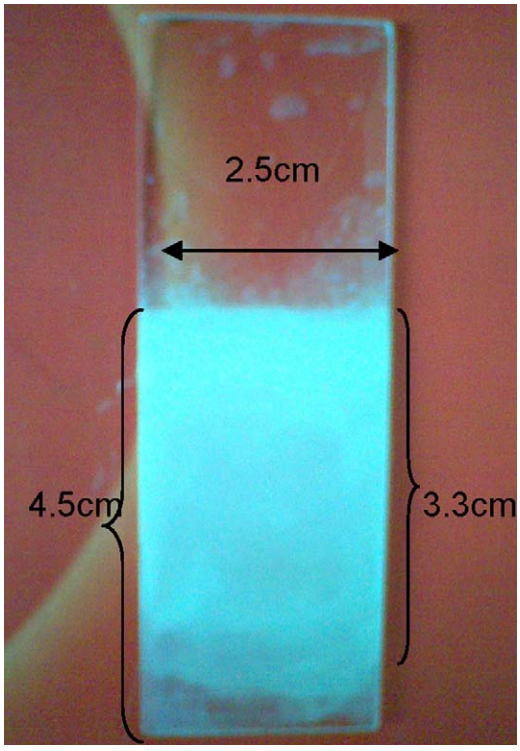

Fig. 7. The area of film covered on the glass.

Table 1
The recycling photodegradation rate (%) of SiTiA film.

Samples	1	2	3	4
SiTiA	96.7	96.0	95.2	96.1
SiTiB	96.7	95.5	93.0	90.0

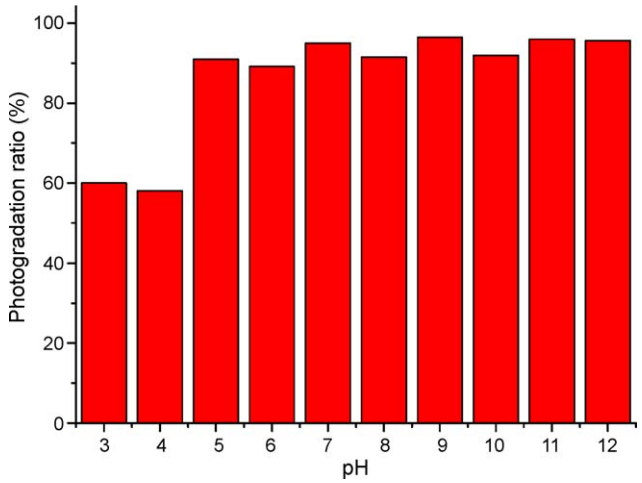

Fig. 9. The effect of pH on methylene blue degradation.

SiO_3^{2-} doped TiO_2 film of SiTiB film (Fig. 8c) is thinner than SiTiA film (Fig. 8b). Therefore, the photocatalytic activity of SiTiB film (Fig. 8c) is not advanced. The photocatalytic activity of SiTiA film (Fig. 8a) without light cutoff filter is better than SiTiA film (Fig. 8b) with cutoff filter. That illustrates that SiO_3^{2-} doped TiO_2 film can also absorbed UV light. The photocatalytic activity of SiTiA film (Fig. 8e) is a little worse than SiTiA film (Fig. 8b). That is because that SiTiA film (Fig. 8b) with the morphology of nanoneedle had lager surface than SiTiA film (Fig. 8e) with the morphology of nanorectangle block.

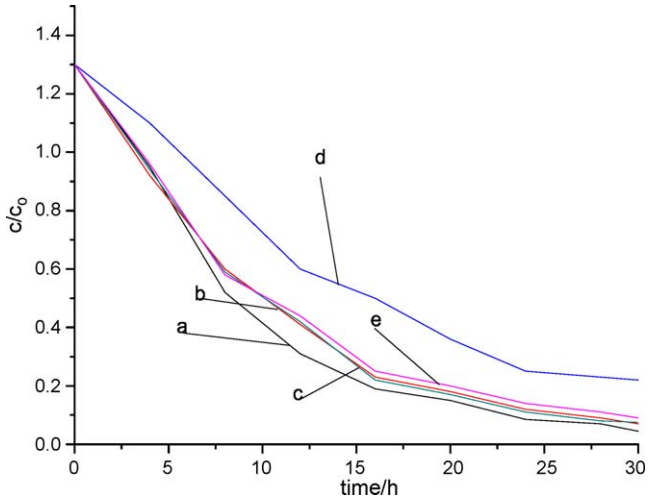

Fig. 8. Photodegradation of methylene blue by using (a) SiTiA film without cutoff filter. (b) SiTiA film prepared with a lot of O_2 with cutoff filter. (c) SiTiB film with cutoff filter. (d) P-25 with cutoff filter. (e) SiTiA film prepared with a little of O_2 with cutoff filter.

Table 1 illustrates that the average of the four times recycling photodegradation rate of SiTiA film prepared with a lot of O_2 is about 96.0%. Photocatalytic activity of the film is very stable after 4 times recycling. However, photocatalytic activity of SiTiB film is decreased. Because the interface of two layers is not stable when immersed in methylene blue for long time.

3.8. Effect of pH

The pH of the solution is one of the most important controlling parameters in the degradation of methylene blue on semiconductor metal oxides. The wastewater from textile industries usually has a wide range of pH values. When $pH > 5$, the percentage of degradation is stable; while $pH < 5$, the percentage of degradation decreases (Fig. 9). PH effect can be explained on the basis of point of zero charge of SiO_3^{2-} doped TiO_2. The PH_{pzc} of SiO_3^{2-} doped TiO_2 is above 4.0. At pH values higher than 4.0, the surface become negative charge, and the opposite occurs for pH values greater than PH_{pzc}. Since methylene blue is a cationic dye, it is conceivable that high pH adsorption is favored on a positively charged surface and hence the reaction is faster at alkaline pH.

4. Conclusions

SiO_3^{2-} doped TiO_2 films with oriented nanoneedle and nanorectangle block structure has been firstly successfully fabricated by hydrothermal synthesis method. XRD results demonstrate that the SiO_3^{2-} doped TiO_2 films are rutile and brookite phases. The SEM analysis reveals that the quantity of O_2 affects the morphology of the SiTiA films films. The films

are very vicelike and the thickness is about 8 μm. SiTiB films with modified substrate display two layers, one is porous structure, the other is nanoneedle structure. UV–vis, IR, TEM and EDX all prove that SiO_3^{2-} have been doped in the TiO_2 crystal structure. They have remarkable red shift and higher photocatalytic activity of degradation of methylene blue than P-25 under visible light ($\lambda > 420$ nm) irradiation. Besides, photocatalytic activity of the film is stable during 4 times recycling. Analyse the reaction mechanism and conform that Ti (III), stable acid radical and O_2 are the crucial elements in fabricating the film. This SiO_3^{2-} doped TiO_2 films will be very useful as photocatalyst to settle various environmental problems, because the present hydrothermal synthesis technique is very simple and inexpensive, meanwhile the material and substrate are very cheap.

References

[1] T. Yazawa, F. Machida, K. Oki, A. Mineshige, M. Kobune, Novel porous TiO_2 glass–ceramics with highly photocatalytic ability, Ceram. Int. 35 (2009) 1693–1697.

[2] R.D. Sun, A. Nakajima, A. Fujishima, T. Watanabe, K. Hashimoto, Photoinduced surface wettability conversion of ZnO and TiO_2 thin films, J. Phys. Chem. B 105 (2001) 1984–1990.

[3] N.A. Sakai, Fujishima, T. Watanabe, K. Hashimoto, Enhancement of the photoinduced hydrophilic conversion rate of TiO_2 film electrode surfaces by anodic polarization, J. Phys. Chem. B 105 (2001) 3023–3026.

[4] D. Kuščer, M. Kosec, J. Holc, Correlation between sintering conditions and water contact angles for Ti–O thick films screen printed on an alumina substrate, Ceram. Int. 35 (2009) 1063–1069.

[5] H.J. Nam, T. Amemiya, M. Murabayashi, K. Itoh, Photocatalytic activity of sol–gel TiO_2 thin films on various kinds of glass substrates: the effects of Na^+ and primary particle size, J. Phys. Chem. B 108 (2004) 8254–8259.

[6] J.C. Yu, W.Ho. Lin, J.H. Yip, P.K. Wong, Photocatalytic activity, antibacterial effect, and photoinduced hydrophilicity of TiO_2 films coated on a stainless steel substrate, Environ. Sci. Technol. 37 (2003) 2296–2301.

[7] H. Tian, J. Ma, K. Li, J. Li, Hydrothermal synthesis of S-doped TiO_2 nanoparticles and their photocatalytic ability for degradation of methyl orange, Ceram. Int. 35 (2009) 1289–1292.

[8] N. Laugel, J. Hemmerlé, N. Ladhari, Y. Arntz, E. Gonthiera, Y. JC, Composite films of polycations and TiO_2 nanoparticles with photoinduced superhydrophilicity, J. Colloid Interface Sci. 324 (1–2) (2008) 127–133.

[9] F. Sayılkan, M. Asiltürk, N. Kiraz, E. Burunkaya, Photocatalytic antibacterial performance of Sn^{4+}-doped TiO_2 thin films on glass substrate, J. Hazard. Mater. 162 (2009) 1309–1316.

[10] K.M. Parida, N. Sahu, N.R. Biswal, B. Naik, A.C. Pradhan, Preparation, characterization, and photocatalytic activity of sulfate-modified titania for degradation of methyl orange under visible light, J. Colloid Interface Sci. 318 (2) (2008) 231–237.

[11] X Xu, S. Li, X. Li, J. Gu, Fe. Chen, X. Li, H. Li, Degradation of n-butyl benzyl phthalate using TiO_2/UV, J. Hazard. Mater. 164 (2009) 527–532.

[12] S. Yin, Q.W. Zhang, F. Saito, T. Sato, Polarised photofluorescence excitation spectroscopy: a new technique for the study of molecular photodissociation. Photolysis of H_2O in the vacuum ultraviolet, Chem. Phys. Lett. 32 (2003) 358–359.

[13] S.U.M. Khan, M. Al-Shahry, W.B. Ingler, Efficient photochemical water splitting by a chemically modified n-TiO_2, Science 297 (2002) 2243–2245.

[14] R. Asahi, T. Morikawa, T. Ohwaki, K. Aoki, Y. Taga, Visible-light photocatalysis in nitrogen-doped titanium oxides, Science 293 (2001) 269–271.

[15] J.L. Gole, J. Stout, C. Burda, Y. Lou, X. Chen, Highly efficient formation of visible light tunable $TiO_{2-x}N_x$ photocatalysts and their transformation at the nanoscale, J. Phys. Chem. B 108 (2004) 1230–1240.

[16] U. Sandro, D. Alessandro, S. Domenica, B. Silvia, Z. Adriano, L. Carlo, $(I_2)_n$ encapsulation inside TiO_2: a way to tune photoactivity in the visible region, J. Am. Chem. Soc. 129 (2007) 2822–2828.

[17] W. Su, Y. Zhang, Z. Li, L. Wu, X. Wang, J. Li, X. Fu, Multivalency iodine doped TiO_2: preparation, characterization, theoretical studies, and visible-light photocatalysis, Langmuir 24 (2008) 3422–3428.

[18] J Yu, S. Liu, Z. Xiu, W. Yu, G. Feng, Synthesis of sulfur-doped TiO_2 by solvothermal method and its visible-light photocatalytic activity, J. Alloys Comd. 471 (1–2) (2009) L23–L25.

[19] M.C. Bolunt, D.H. Kim, J.L. Falconer, Transparent thin-film TiO_2 photocatalysts with high activity, Environ. Sci. Technol. 35 (2001) 2988–2994.

[20] C. Lu, C. Hu, C. Wu, Low-temperature preparation and characterization of iron-ion doped titania thin films, J. Hazard. Mater. 159 (2008) 636–639.

[21] L. Mi, P. Xu, P. Wang, Experimental study on the bandgap narrowings of TiO_2 films calcined under N_2 or NH_3 atmosphere, Appl. Surf. Sci. 255 (5) (2008) 2574–2580.

[22] H. Eiji, F. Shinobu, K. Keita, Growth of submicrometer-scale rectangular parallelepiped rutile TiO_2 films in aqueous $TiCl_3$ solutions under hydrothermal conditions, J. Am. Chem. Soc. 126 (2004) 7790–7791.

[23] W. Ho, C.Yu. Jimmy, J. Yu, Photocatalytic TiO_2/glass nanoflake array films, Langmuir 21 (2005) 3486–3492.

[24] A. Duran, C. Serna, V. Fornes, J.M.J. Fernandez-Navarro, Structural considerations about SiO_2 glasses prepared by sol–gel, Non-Cryst. Solids 82 (1–3) (1986) 69–77.

[25] D.C.M. Dutoit, M. Schmeider, A. Baiker, Titania–silica mixed oxides. I. Influence of sol–gel and drying conditions on structural properties, J. Catal. 153 (1) (1995) 165–176.

[26] M. Zhang, L. Shi, Y. Shuai, Y. Zhao, J. Fang, A novel route to prepare pH- and temperature-sensitive nanogels via a semibatch process, J. Colloid Interface Sci. 330 (2) (2009) 113–118.

[27] H. Zhang, Q. Xie, S. Chen, H. Zhao, Fabrication and characterization of silica/titania nanotubes composite membrane with photocatalytic capability, Environ. Sci. Technol. 40 (2006) 6104–6109.

[28] D. Wang, J. Liu, Q. Huo, Z. Nie, W. Lu, E. Rick, Surface-mediated growth of transparent, oriented, and well-defined nanocrystalline anatase titania films, J. Am. Chem. Soc. 128 (2006) 13670–13671.

[29] H. Eiji, F. Shinobu, I. Hiroaki, H. Itaru, M. Ichihara, H. Zhou, One-step synthesis of nano–micro chestnut TiO_2 with rutile nanopins on the microanatase octahedron, Acs Nano 1 (2007) 273–278.

[30] S. Mukai, H. Nishihara, S. Shichi, H. Tamon, Preparation of porous TiO_2 cryogel fibers through unidirectional freezing of hydrogel followed by freeze-drying, Chem. Mater. 16 (2004) 4987–4991.